Chapter 12: Biological characterization of nanomaterials

Anita Jemec, Tina Mesarič, Maja Sopotnik, Kristina Sepčić, Damjana Drobne

University of Ljubljana, Biotechnical Faculty, Department of Biology, Večna pot 111, SI-1000 Ljubljana, Slovenia

12.1 Introduction

12.1.1 Importance of nanomaterial (NM) characterisation

The safety of nanotechnology products is seen as a crucial element in ensuring that the benefits of nanotechnology outweigh the potential risks of nanomaterials (NMs). A large number of nanosafety related projects have been launched in the past. For example, only in the EU about fifty projects are either completed or running and represent a total RTD investment of € 137 M under FP6 (13 projects, € 31 M) and FP7 (34 projects, € 106 M) (http://www.nanosafetycluster.eu). Recently, a list of NM physicochemical properties most relevant for NM preparation and safety testing has been suggested by experts from the EU Nanosafety cluster working group 10 on integrated approaches to testing and assessment [1]. These properties are: (a) composition, (b) impurities, (c) size/shape/and size distribution, (d) surface area, (e) surface chemistry/crystallinity/reactivity/coating, (f) pH, and (g) solubility/dissolution.

In the past decade it has become clear in nanotoxicology research that the reporting of physicochemical characteristics of NMs is necessary to aid the hazard identification of nanomaterials [2–4]. The ability to establish the relationship between the NMs' properties and the

observed biological responses will enable the grouping of hazard NMs according to their specific properties. However, establishing this correlation is not trivial and the challenges associated have been previously discussed by several researchers [5–7]. Particle size and surface area are considered important factors for determining the toxicity of particles; such observation was reported for algae exposed to SiO_2 [8]. Another property of relevance to consider is the surface area, which is not surprising, as there is a correlation between the two properties, i.e. when the particle size decreases, the surface area increases. Therefore, NMs with a small particle size (and hence a larger surface area) are often expected to provoke a higher toxicity. In addition to these two properties, the surface texture and the crystallinity of NMs can also play a role. For example, the toxicity of large textured ZnO nanoparticles (NPs) to inflammatory cells (macrophage-derived cells RAW 264.7 cell line) is higher than that of much smaller sized (5 nm), low crystallinity nanoparticles [9]. Furthermore, the shape of the nanomaterial has shown to affect the toxicology response e.g. as in Ag NPs with the gram-negative *E. coli* [10]. Although several past researchers have identified several parameters that can be correlated to a biological response, the larger picture may be that the toxicity can only be explained by the integrated effect of multiple properties, i.e. a set of secondary properties, which has been referred to as "extrinsic NMs' characteristics in the biological system" [1, 11, 12].

12.1.2 Extrinsic NMs characterisation

The most prominent trait of NMs is that they are not static when entering a biological environment and that their subsequent modifications will result in them acquiring new "extrinsic" properties. NMs acquire new extrinsic properties, which result in different forms of material. These changes can occur either instantly or during their lifetime, upon them entering the

biological environments; the latter phenomenon is referred to as the aging of NMs [13]. Several interactions between the nanomaterial and the environment can occur as a result of a combination of several different factors rather than just a single factor. Several factors governing the interactions include: ionic strength, pH, and media composition (e.g. presence of natural organic matter, polysaccharides, proteins, specific counter ions, such as Ca^{2+} and Mg^{2+}) [13, 14], colloidal stability, which in turn will be governed by the coatings on the nanomaterial and stabilizing agents [3]. Furthermore, aggregation, flocculation, redox reactions, dissolution, reaction with reduced sulfur species or chloride, photooxidation, photoreduction, adsorption of polymers or natural organic matter and interaction with essential metals, like Ag NPs with selenium [15] can also occur [16]. The different factors listed here can result in the nanomaterial acquiring extrinsic properties.

A well-known phenomenon of NMs is their readiness to interact with biomolecules [17], resulting in the formation of non-covalent bonds between them [7]. In biological fluids, NMs are known to interact with phospholipids, proteins, DNA, and small metabolites [18] and there is increasing evidence of rapid formation of the so-called "protein corona," i.e. the coating of protein molecules around the NMs [7, 19]. The formation of NMs' bio-complexes originating from the adsorption of various components in a biological environment, independent of proteins has also been recorded; due to salts, these nano-bio complexes originated from the test medium [20].

Due to the inherent complexity of nanomaterial interactions in the biological medium and the subsequent modifications of the NMs, the physicochemical characterisation of NMs *in situ* is a difficult analytical challenge, which requires a multi-method approach [21, 22]. The complicated interactions and dynamic changes of NMs mean that it is difficult to make a

meaningful characterization of NMs physicochemical properties [19]. In addition, Tantra et al. [23] discussed difficulties in making a reliable measurement with the current instrumentation, specifically when the NMs are in complex media. The main sources of potential experimental errors identified by Tantra et al. [23] included the (high) polydispersity of nanomaterials and the complex environment the nanomaterial is in. Subsequently, this often resulted in employing methods that did not fit the purpose. According to Baalousha and Lead [24], most of the materials tested in nanotoxicology research are considered far too polydisperse to be appropriate for current analytical techniques [24]. Another issue which arises when the nanomaterials are in complex media is the creation of an unstable environment, resulting in NMs to agglomerate and/or sediment. Under such conditions, the measurements may be very unreliable. Furthermore, in relation to bioassay measurements, a number of other interferences that may result in making an unreliable measurement may appear, e.g. the contamination of NMs, interference with the assay readout, and variations in dispersion protocols [23].

12.1.3 The proposal for measuring "extrinsic" properties

It is clear that a high level of overarching property to describe nanomaterial interactions with biological environment is much needed [25]. In this chapter, such new approach, based on biological characterisation and the measurement of extrinsic properties, will be presented. The idea is based on the knowledge that NM properties, such as the size, surface chemistry, crystallinity, and hydrophobicity, govern the adsorption potential of NMs, which is reflected in the interaction of NMs with the biological system, specifically, a protein biosensor system that is able to quantify these interactions will be presented.

The chapter is divided into several sections: a) a general introduction on the existent approaches to describe the integrated surface properties; b) the quantification of interactions between NMs and proteins, as novel proposed tools); c.) an experimental case study that employs the use of acetylcholinesterase (AChE) based biosensor (used to rank different carbon based NMs based on their adsorption and interactions with this enzyme).

12.2 Measurement methods

12.2.1 Review of existing approaches

An attempt to use extrinsic properties to describe NM interaction with biological media has been discussed by Xia et al. [19]. In particular, a biological surface adsorption index (BSAI) based on computer simulations has been proposed to describe the surface adsorption energy of NMs under biologically relevant aqueous conditions. The BSAI is an integrative measure of the surface adsorption energy of NMs and is derived from 5 diverse nanodescriptors representing molecular forces of NM interaction with biological system: lipophilicity, hydrogen-bond basicity and acidity, dipolarity/polarizability and lone-pare electrons. The limitation of this model is the assumption of idealized biological conditions, where the interaction is based on the estimation of how biomolecules may interact with the surface of NMs, rather than a direct experimental measurement of their interactions.

Another approach employed to characterize the extrinsic surface properties of NMs is the quantification of the interactions between NMs and proteins [26]. As discussed above, such interactions are complex and dynamic. Upon the interactions of NMs with proteins, a number of

phenomena can be monitored to measure the extent of such interactions: (a) the binding affinity of NMs [18], (b) the NM-protein binding kinetics, followed by surface plasmon resonance [18, 27], (c) the stoichiometry of interaction [28], (d) the identification of the binding sites of NMs [29], (e) protein conformational changes [30–34], (f) protein stability, and (g) proteins function changes [31–34]. The latter refers to changes in enzyme activity and the adsorption of NMs onto the protein. This approach has been previously successfully used to investigate the effects of carbon-based NMs and it will be presented in the following experimental case study [31]. In this work, the recombinant enzyme acetylcholinesterase (AChE) purified from the fruit fly (*Drosophila melanogaster*) was used as the model protein.

12.2.2 Introducing acetylcholinesterase as a model biosensor protein

Acetylcholinesterase (AChE) (E.C.3.1.1.7) belongs to the family of cholinesterases, which are carboxylic ester hydrolases that break down esters of choline. In vertebrates, AChE is mainly found at neuromuscular junctions and cholinergic synapses in the central nervous system, where it is responsible for the hydrolysis of acetylcholine into choline and acetate after the activation of acetylcholine receptors at the postsynaptic membrane and thus essential for the proper functioning of the central and the peripheral nervous systems [35, 36]. It is also found in red blood cell membranes, where its physiological role is to date unknown [37].

The hydrolysis of acetylcholine happens at the catalytic site of the enzyme, which is deeply buried, located at the bottom of a 20 Å long and narrow cavity, called the active-site gorge. The gorge is covered by as many as 14 conserved aromatic residues covering by over 70 % of its surface [38]. In addition, all known AChEs include a secondary substrate-binding site, referred to as the peripheral anionic site. This site is involved in several functions, such as the

modification of catalytic activity, the mediation of interaction of AChE with inhibitors and the non-catalytic role, namely β-amyloid fibril formation [39].

In general, AChEs are specifically inhibited by organophosphates (OP) and carbamates (CA) [36, 40]. The proposed mechanism of inhibition is binding to the serine hydroxyl group at the active site, and this binding is much stronger than the binding of acetylcholine. In addition, AChEs are also inhibited by other types of pollutants, such as metals [41–43], other pesticides [44], polycyclic aromatic hydrocarbons, detergents [36, 45] and more recently NMs [31, 32]. In relation to metal inhibition, the proposed mechanism of action for metal inhibition lies in the alteration of AChE's binding properties for acetylcholine [46]. It has also been suggested that the conformation of AChE is highly responsive to even subtle changes in ionic composition. The influence of ions on AChE conformation might arise from ion association with the peripheral anionic site, which seems to interact with the anionic site that resides inside the AChE active site gorge [47].

As pointed out by Lionetto et al. [36] the successful application of AChEs as biomarkers for use in the occupational and environmental risk assessment can be attributed to: the ease of measurement, the dose-dependent response to pollutants, the high level of sensitivity and links at an organism level. These properties are also the reason for the wide application of AChE in biosensors. As a result, numerous cholinesterase-based biosensors with various enzyme sources, detection and immobilization methods have already been developed [48, 49].

12.3 Experimental Case Study

12.3.1 Introduction

Carbon-based nanomaterials have emerged in recent years as promising candidates for drug delivery systems, cellular imaging, biosensor matrices, and other biomedical applications. Carbon-based nanomaterials comprise a variety of different NMs with very different properties. Among them are: fullerenes (C_{60}), graphene-family nanomaterials, and carbon black. Graphene is a single-atom thick, two-dimensional sheet of hexagonally arranged carbon atoms isolated from its three-dimensional parent material, graphite. Related materials include few-layer-graphene, ultrathin graphite, graphene oxide (GO), reduced graphene oxide, and graphene nanosheets. GO has unique structural, mechanical and electronic properties and is used in bio-devices [50, 51]. Fullerenes are carbon allotropes similar in structure to graphene but rolled up to form closed-cage, hollow spheres. The C_{60} fullerene is a remarkably stable compound consisting of 60 carbon atoms [52]. They have been mass-produced for many applications in recent decades, including targeted drug delivery, polymer modifications and cosmetic products, energy storage, sensors, and semiconductors [53]. Carbon black is produced from incomplete combustion and is an amorphous carbon material with a high surface-area-to-volume ratio. The three NMs differ in their hydrophobicity; while GO is amphiphilic due to the presence of epoxide and hydroxyl groups on the surface, CB and C_{60} are hydrophobic.

Adsorption of proteins on carbon-based NMs has been extensively studied and it was shown that these interactions can affect both the protein structure and function [30, 54]. Hydrophobic interactions, π–π stacking interactions, and electrostatic interactions are reported to play key roles in the binding of proteins to NMs [54]. Recent molecular dynamics (MD) studies have, for example, shown that both carbon nanotubes and graphene have the capability to disrupt

α-helical structures of short peptides and that graphene may possess even a higher capability to break α-helices due to its more favourable surface curvature [30].

The aim of this study is to present an example of the interaction between carbon-based NMs (carbon black (CB), graphene oxide (GO) and fullerenes (C_{60})) and recombinant AChE (from fruit fly (*Drosophila melanogaster*)). This particular AChE was chosen as the model system, since it has a well-known structure. The adsorption and inhibition of AChE activity reported will present measures of its interaction with carbon-NMs. The data presented here is based on the data previously reported by Mesarič et al. [31].

12.3.2 Method: Assay of AChE activity

The measurement of AChE activity was done according to the most widely applied method by Ellman [55], adapted for microplates. AChE hydrolyzes the substrate acetylthiocholine chloride to produce thiocholine and acetate. The thiocholine in turn reduces the color indicator (5,5'-dithiobis-(2-nitrobenzoic acid)) acid liberating 3-thio-6-nitrobenzoate. The formation of this chromogenic product is followed at 405 nm and the rate of formation is considered related to the activity of the AChE. Fig. 12-1 shows a schematic of the overall reaction.

Figs. 12-2 and 12-3 show an illustration of different steps associated with adsorption and inhibition experiments, respectively. Please note that there are differences between the two types of experiments. In the case of inhibition experiments, the activity of total AChE (the NMs-bound and "free" AChE) was measured, because the reagents were added to the AChE-NMs incubation mixture, prior to the separation of AChE-NMs complexes. On the other hand, in the case of

adsorption experiments, the activity of "free" AChE is measured and subtracted from the total (free and NMs- bound) AChE to evaluate the adsorbed share of AChE.

The inhibition experiment was set up in the following way: the *D. melanogaster* AChE (50 µl of AChE dissolved in 100 mM phosphate buffer; pH 8.0; 0.06 U/ml) was first incubated with 10 µL of NMs' suspension in the same buffer (final concentrations in the range of 0-1 mg/mL). After 10 min of incubation between AChE and NMs, 100 µL of Ellman's reagent and 50 µL of the substrate acetylthiocholine chloride (2 mM) were added. This reagent mixture was incubated for another 5 min. The NM-AChE complexes were then separated by centrifugation (5 min at 12,000 g). The supernatants (210 µL) were pipetted onto a microtiter plate and the absorbance was measured at 405 nm exactly 20 min after the addition of the substrate and the Ellman's reagent to the reaction mixture, using the automatic VIS microplate reader (Dynex technologies, USA). For every sample that contained NMs, an appropriate blank was prepared, where the enzyme was replaced by 50 µL of 100 mM phosphate buffer pH 8.0 (Fig. 12-2).

The adsorption procedure was as follows: AChE was incubated with the NMs for 2 min using the same volumes of AChE and NMs as in the case of inhibition experiments. Afterwards, the sample was centrifuged (4 min at 12,000 g) and the supernatants (60 µL), containing the non-adsorbed "free" enzyme, were pipetted onto the microtiter plate. The reagents (100 µL of Ellman's reagent and 50 µL of 2mM substrate) were added only to the supernatant. In this case, the activity of free, non NMs-adsorbed AChE was read at 405 nm exactly 20 min after the addition of the substrate and Ellman's reagent to the reaction mixture (Fig.12-3).

The interference of NMs with the reaction product (3-thio-6-nitrobenzoate) was evaluated. For this purpose, 5,5'-dithiobis-(2-nitrobenzoic acid) was reduced with a minimal volume of 2-mercaptoethanol to obtain the 3-thio-6-nitrobenzoate. It was diluted to give the final value of absorbance at 405 nm, identical to the one obtained in the enzyme reaction without the NM. 100

μL of such solution was combined with 50 μL of 2 mM substrate, 50 μL of 100 mM phosphate buffer (pH 8.0) and 10 μL of the appropriate NM suspension. The absorbance was read at 405 nm to check for changes in the color; no interference of NMs with the test assay was found.

12.3.3 Results and discussion

Table 12-1 shows a summary of the results. As mentioned before, the work has been previously published and details can be found elsewhere [31]**.** Based on the IC_{20} values (this is the concentration that causes 20 % of the changes in comparison to control), the NMs can be ranked in the order from the least to the most AChE-adsorptive and inhibitory. The NM with a lower IC_{20} is considered more adsorptive/inhibitory. Results show that GO and CB exhibited similar adsorption and inhibition properties. Although GO shows a slightly higher adsorptive/inhibitory potential than CB, it is clear that they both have a significantly higher adsorption and inhibition than C_{60}.

Table 12-1 shows the inherent differences between the physicochemical properties of the three NMs, which may explain their adsorptive/inhibitory potentials. It is clear that there is no evidence that links particle size with adsorptive/inhibitory potentials. Although GO has similar adsorptive/inhibitory potentials to CB, the particle sizes (both primary and secondary particles) are very different.GO is an 80 % single sheet with a size of 0.5–5 μm, whereas carbon black is amorphous and globular, with a primary size of 20 nm. In test media, aggregates of carbon black in the range of 100 nm–1 μm are present.

Out of the different properties noted in Table 12-1, there is some indication that surface curvature may play an important role. Here, GO and CB both exhibit a low surface curvature, while the opposite is true for C_{60}. The high surface curvature of C_{60} could explain its low adsorption/inhibition to the enzyme. Another difference between the materials concerns hydrophobicity. While GO is amphiphilic, i.e. possesses both hydrophilic and hydrophobic residues due to the presence of epoxide and hydroxyl groups on the surface, CB and C_{60} are hydrophobic in nature. These differences, however, do not affect their adsorption/inhibition properties, since GO is similarly affected by AChE as CB despite the different hydrophobicity properties. Clearly, the study presented here is preliminary in nature and a clearer link between the observed effects of AChE and the aforementioned properties can be established if a larger set of data is acquired, e.g. investigating the interaction of different NMs with AChE (of different isoforms and from different sources).

In an attempt to elucidate the reasons behind the observed differences in AChE inhibitions, Mesarič et al. [31] performed computational simulation studies to investigate the probable adsorption site of AChE on the surface of carbon NMs. Results from the simulation study showed that: a) in most of the cases, the interaction site of AChE with carbon-based NMs is far from the active site of the enzyme, b) CB seems to form more atomic contacts than GO and C_{60}, c) the hydrophobic binding of CB affects the secondary structure of the enzyme. However, the results of the simulation do not seem to give any explanation as to the results reported here. For example, CB and GO have a quite similar adsorption/inhibition potential (Table 12-1), so the number of atomic contacts does not influence the inhibition.

To date, a similar study has been published by Wang and co-workers [32]. Their study differs in that they have used AChE from another source (i.e. electric eel) and applied a longer

incubation time of NMs with AChE (15 min). Their findings indicated a higher adsorption potential of carbon NMs in comparison to metal oxide NMs (SiO_2, TiO_2) (15 min IC_{50}>800 mg/L) [32]. They also suggested that special attention should be paid to those metal oxide NMs where metals dissolve and metal ions are the source of inhibition (as, for example, Cu^{2+} in the case of Cu nanoparticles). Their results concur with the modelled adsorption potentials introduced by Xia et al. [19], where carbon NMs were ranked as significantly more adsorptive than metal oxide NMs (SiO_2, Ag-SiO_2, and TiO_2). The model introduced by Xia has been employed for the three NMs in this study, but findings suggest that it does not predict the differences between them.

	PHYSICO-CHEMICAL PROPERTIES	**INHIBITION OF ACTIVITY (mg/l, time of incubation is noted)**	**ADSORPTION EFFICIENCY (mg/l; time of incubation is noted)**
Graphene oxide (GO)	- 80 % single sheet, sheet size varies from 0.5 to 5 μm - secondary size in test media: DLS analysis not possible - ***low*** surface curvature - ***amphiphilic*** nature: presence of epoxide and hydroxyl groups on the surface	10 min IC_{20} = 0.057 ± 0.008	2 min IC_{20} = 0.005 ± 0.001

Carbon black (CB)	- amorphous, globular - primary size: 13 nm - secondary size in test media (100 nm–1 μm range) - ***low*** surface curvature - ***hydrophobic*** nature	10 min IC_{20} = 0.15 ± 0.04	2 min IC_{20} = 0.06 ± 0.01
Fullerene (C_{60})	- primary size distribution (20 nm to several 100 nm) - secondary size in test media (250 nm to several μm) - ***high*** surface curvature - ***hydrophobic*** nature	10 min IC_{20} = 40 ± 5	2 min IC_{20} = 30 ± 5

Table 12-1. Summary of data: the physicochemical properties of NMs, their AChE inhibition and adsorption potentials to recombinant AChE (from *Drosophila melanogaster*); further details can be found elsewhere [31]. The arrow indicates an increase in adsorption and inhibition.

Finally, it is important to point out that the data presented in this work refers specifically to the recombinant AChE from *Drosophila melanogaster*. Although the differences in the three-dimensional structure of AChE from different species are not significant, some subtle differences are present, which may result in different inhibitor susceptibility [56]. For example, although the comparison of AChE purified from the Pacific electric ray (*Torpedo californica*), the human and

the mouse revealed no conformational differences within the active-site gorge or in the composition of its surface residues, there were differences related to the layers behind those lining the active site[57]. Also, differences between the *Drosophila melanogaster* AChE and AChE from the human, the mouse, and the fish were not found in the overall fold, charge distribution, and deep active-site gorge, but in the external loops and in the tilt of the C-terminal helix [58]. Furthermore, the active-site gorge of the insect enzyme is significantly narrower than that of the *Torpedo californica* AChE and its trajectory is shifted by several angstroms [58]. Marked structural differences are also found between different AChE isoforms, for example between the erythrocytic and synaptic variant [39]. Overall, this indicates that the interaction (adsorption and inhibition) of NMs with different variants of AChE from different species may vary.

12.3.4 Conclusions

In conclusion, a novel type of NM characterisation has been presented, i.e. a biological characterisation using an enzyme biosensor. Using the current model based specifically on recombinant AChE from the fruit fly (*Drosophila melanogaster*), three carbon-based NMs were ranked according to their adsorptive and inhibitory properties. These results suggest a promising use of the proposed biosensor for ranking NMs with regard to their hazard. The results presented here are preliminary in nature and further work is undoubtedly needed in order to establish a clear link between their properties and the biological response. Furthermore, for a successful uptake of this new tool for characterizing nanomaterials, it is important to validate the method, e.g. investigate the effect of the different sources (and isoforms) of AChE, the different incubation

periods of NMs with the enzymes, and the interaction with a variety of NMs (with variable properties). Only after an acquisition of a larger set of data on the interaction of different NMs with different forms of AChE has been accomplished, will it be possible to connect the observed effects of AChE on the extrinsic properties of NMs.

12.4 Summary

The characterisation of nanomaterials is of crucial importance in ranking NMs according to their hazard. In real biological systems, nanomaterials undergo complex modifications, thus potentially gaining what has been referred to as secondary, "extrinsic" properties. Due to the difficulties in making reliable measurements of NMs when in complex media, the characterization of NMs under such conditions can be a challenging task. In this study, an overarching concept of NM characterization has been put forward, based on a biological characterization approach using an enzyme biosensor. The idea is based on the knowledge that the properties of NMs, such as size, surface chemistry, crystallinity, and hydrophobicity, govern their adsorption potential, which is reflected in their interaction with biological systems, specifically with proteins. It has been shown that the biosensor system is able to quantify these interactions. Results show that AChE is a promising candidate for ranking different NMs according to their adsorptive and inhibitory properties.

Acknowledgements

This research was funded by the EU FP7 project NanoValid (Development of reference methods for hazard identification, risk assessment, and LCA of engineered nanomaterials; Grant

No 263147) and NanoMile (NMP4-LA-2013-310451). We thank the editor for valuable suggestions in preparation of this manuscript.

References

1. A. G. Oomen, P. M. J. Bos, T. F. Fernandes, K. Hund-Rinke, D. Boraschi, H. J. Byrne, K. Aschberger, S. Gottardo, F. von der Kammer, D. Kühnel, D. Hristozov, A. Marcomini, L. Migliore, J. Scott-Fordsmand, P. Wick, and R. Landsiedel, "Concern-driven integrated approaches to nanomaterial testing and assessment – report of the NanoSafety Cluster Working Group 10," *Nanotoxicology*, **8**, 3, 334–348 (2014).

2. A. Menard, D. Drobne, and A. Jemec, "Ecotoxicity of nanosized TiO2. Review of in vivo data," *Environ. Pollut.*, **159**, 3, 677–684 (2011).

3. D. R. Hristozov, A. Zabeo, C. Foran, P. Isigonis, A. Critto, A. Marcomini, and I. Linkov, "A weight of evidence approach for hazard screening of engineered nanomaterials," *Nanotoxicology*, **8**, 1, 72–87 (2014).

4. D. Kühnel and C. Nickel, "The OECD expert meeting on ecotoxicology and environmental fate — Towards the development of improved OECD guidelines for the testing of nanomaterials," *Sci. Total Environ.*, **472**, 347–353 (2014).

5. A. Kahru and H.-C. Dubourguier, "From ecotoxicology to nanoecotoxicology," *Toxicology*, **269**, 2–3, 105–119 (2010).

6. G. Oberdörster, E. Oberdörster, and J. Oberdörster, "Nanotoxicology: An Emerging Discipline Evolving from Studies of Ultrafine Particles," *Environ. Health Perspect.*, **113**, 7, 823–839 (2005).

7. A. Nel, T. Xia, L. Mädler, and N. Li, "Toxic Potential of Materials at the Nanolevel," *Science*, **311**, 5761, 622–627 (2006).

8. K. Van Hoecke, K. A. C. De Schamphelaere, P. Van der Meeren, S. Lcucas, and C. R. Janssen, "Ecotoxicity of silica nanoparticles to the green alga pseudokirchneriella subcapitata: Importance of surface area," *Environ. Toxicol. Chem.*, **27**, 9, 1948–1957 (2008).

9. A. A. Selim, A. Al-Sunaidi, and N. Tabet, "Effect of the surface texture and crystallinity of ZnO nanoparticles on their toxicity," *Mater. Sci. Eng. C*, **32**, 8, 2356–2360 (2012).

10. S. Pal, Y. K. Tak, and J. M. Song, "Does the Antibacterial Activity of Silver Nanoparticles Depend on the Shape of the Nanoparticle? A Study of the Gram-Negative Bacterium Escherichia coli," *Appl. Environ. Microbiol.*, **73**, 6, 1712–1720 (2007).

11. A. Jemec, P. Djinović, T. Tišler, and A. Pintar, "Effects of four CeO2 nanocrystalline catalysts on early-life stages of zebrafish Danio rerio and crustacean Daphnia magna," *J. Hazard. Mater.*, **219–220**, 213–220 (2012).

12. I. Lynch, C. Weiss, and E. Valsami-Jones, "A strategy for grouping of nanomaterials based on key physico-chemical descriptors as a basis for safer-by-design NMs," *Nano Today*, **9**, 3, 266–270 (2014).

13. I. A. Mudunkotuwa, J. M. Pettibone, and V. H. Grassian, "Environmental Implications of Nanoparticle Aging in the Processing and Fate of Copper-Based Nanomaterials," *Environ. Sci. Technol.*, **46**, 13, 7001–7010 (2012).

14. M. Hassellöv, J. W. Readman, J. F. Ranville, and K. Tiede, "Nanoparticle analysis and characterization methodologies in environmental risk assessment of engineered nanoparticles," *Ecotoxicology*, **17**, 5, 344–361 (2008).

15. J. Liu, Z. Wang, F. D. Liu, A. B. Kane, and R. H. Hurt, "Chemical Transformations of Nanosilver in Biological Environments," *ACS Nano*, **6**, 11, 9887–9899 (2012).

16. V. K. Sharma, K. M. Siskova, R. Zboril, and J. L. Gardea-Torresdey, "Organic-coated silver nanoparticles in biological and environmental conditions: Fate, stability and toxicity," *Adv. Colloid Interface Sci.*, **204**, 15–34 (2014).

17. S. Park and K. Hamad-Schifferli, "Nanoscale interfaces to biology," *Curr. Opin. Chem. Biol.*, **14**, 5, 616–622 (2010).

18. Q. Mu, G. Jiang, L. Chen, H. Zhou, D. Fourches, A. Tropsha, and B. Yan, "Chemical Basis of Interactions Between Engineered Nanoparticles and Biological Systems," *Chem. Rev.*, **114**, 15, 7740–7781 (2014).

19. X. R. Xia, N. A. Monteiro-Riviere, S. Mathur, X. Song, L. Xiao, S. J. Oldenberg, B. Fadeel, and J. E. Riviere, "Mapping the Surface Adsorption Forces of Nanomaterials in Biological Systems," *ACS Nano*, **5**, 11, 9074–9081 (2011).

20. M. Xu, J. Li, H. Iwai, Q. Mei, D. Fujita, H. Su, H. Chen, and N. Hanagata, "Formation of Nano-Bio-Complex as Nanomaterials Dispersed in a Biological Solution for Understanding Nanobiological Interactions," *Sci. Rep.*, **2**, (2012).

21. J. Fabrega, S. N. Luoma, C. R. Tyler, T. S. Galloway, and J. R. Lead, "Silver nanoparticles: Behaviour and effects in the aquatic environment," *Environ. Int.*, **37**, 2, 517–531 (2011).

22. R. F. Domingos, M. A. Baalousha, Y. Ju-Nam, M. M. Reid, N. Tufenkji, J. R. Lead, G. G. Leppard, and K. J. Wilkinson, "Characterizing Manufactured Nanoparticles in the Environment: Multimethod Determination of Particle Sizes," *Environ. Sci. Technol.*, **43**, 19, 7277–7284 (2009).

23. R. Tantra, C. Oksel, T. Puzyn, J. Wang, K. N. Robinson, X. Z. Wang, C. Y. Ma, and T. Wilkins, "Nano(Q)SAR: Challenges, pitfalls and perspectives," *Nanotoxicology*, 1–7 (2014).

24. M. Baalousha and J. R. Lead, "Nanoparticle dispersity in toxicology," *Nat. Nanotechnol.*, **8**, 5, 308–309 (2013).

25. R. Tantra and A. Shard, "We need answers," *Nat. Nanotechnol.*, **8**, 2, 71–71 (2013).

26. M. P. Monopoli, C. Åberg, A. Salvati, and K. A. Dawson, "Biomolecular coronas provide the biological identity of nanosized materials," *Nat. Nanotechnol.*, **7**, 12, 779–786 (2012).

27. T. Cedervall, I. Lynch, S. Lindman, T. Berggård, E. Thulin, H. Nilsson, K. A. Dawson, and S. Linse, "Understanding the nanoparticle–protein corona using methods to quantify exchange rates and affinities of proteins for nanoparticles," *Proc. Natl. Acad. Sci.*, **104**, 7, 2050–2055 (2007).

28. B. I. Ipe, A. Shukla, H. Lu, B. Zou, H. Rehage, and C. M. Niemeyer, "Dynamic Light-Scattering Analysis of the Electrostatic Interaction of Hexahistidine-Tagged Cytochrome P450 Enzyme with Semiconductor Quantum Dots," *ChemPhysChem*, **7**, 5, 1112–1118 (2006).

29. L. Calzolai, F. Franchini, D. Gilliland, and F. Rossi, "Protein−Nanoparticle Interaction: Identification of the Ubiquitin−Gold Nanoparticle Interaction Site," *Nano Lett.*, **10**, 8, 3101–3105 (2010).

30. G. Zuo, X. Zhou, Q. Huang, H. Fang, and R. Zhou, "Adsorption of Villin Headpiece onto Graphene, Carbon Nanotube, and C60: Effect of Contacting Surface Curvatures on Binding Affinity," *J. Phys. Chem. C*, **115**, 47, 23323–23328 (2011).

31. T. Mesarič, L. Baweja, B. Drašler, D. Drobne, D. Makovec, P. Dušak, A. Dhawan, and K. Sepčić, "Effects of surface curvature and surface characteristics of carbon-based nanomaterials on the adsorption and activity of acetylcholinesterase," *Carbon*, **62**, 222–232 (2013).

32. Z. Wang, J. Zhao, F. Li, D. Gao, and B. Xing, "Adsorption and inhibition of acetylcholinesterase by different nanoparticles," *Chemosphere*, **77**, 1, 67–73 (2009).

33. A. Käkinen, F. Ding, P. Chen, M. Mortimer, A. Kahru, and P. C. Ke, "Interaction of firefly luciferase and silver nanoparticles and its impact on enzyme activity," *Nanotechnology*, **24**, 34, 345101 (2013).

34. G. Šinko, I. V. Vrček, W. Goessler, G. Leitinger, A. Dijanošić, and S. Miljanić, "Alteration of cholinesterase activity as possible mechanism of silver nanoparticle toxicity," *Environ. Sci. Pollut. Res.*, **21**, 2, 1391–1400 (2013).

35. M. Pohanka, “Cholinesterases, a target of pharmacology and toxicology,” *Biomed. Pap.*, **155**, 3, 219–223 (2011).

36. M. G. Lionetto, R. Caricato, A. Calisi, M. E. Giordano, and T. Schettino, “Acetylcholinesterase as a Biomarker in Environmental and Occupational Medicine: New Insights and Future Perspectives,” *BioMed Res. Int.*, **2013**, e321213 (2013).

37. G. Daniels, “Functions of red cell surface proteins,” *Vox Sang.*, **93**, 4, 331–340 (2007).

38. J. L. Sussman, M. Harel, F. Frolow, C. Oefner, A. Goldman, L. Toker, and I. Silman, “Atomic structure of acetylcholinesterase from Torpedo californica: a prototypic acetylcholine-binding protein,” *Science*, **253**, 5022, 872–879 (1991).

39. D. Grisaru, M. Sternfeld, A. Eldor, D. Glick, and H. Soreq, “Structural roles of acetylcholinesterase variants in biology and pathology,” *Eur. J. Biochem.*, **264**, 3, 672–686 (1999).

40. L. G. Sultatos, “Interactions of organophosphorus and carbamate compounds with cholinesterases,” *Toxicol. Organophosphate Carbamate Compd. Elsevier Acad. Press Amst.*, 209–218 (2006).

41. T. C. Diamantino, E. Almeida, A. M. V. M. Soares, and L. Guilhermino, “Characterization of Cholinesterases from Daphnia magna Straus and Their Inhibition by Zinc,” *Bull. Environ. Contam. Toxicol.*, **71**, 2, 0219–0225 (2003).

42. M. F. Frasco, D. Fournier, F. Carvalho, and L. Guilhermino, “Do metals inhibit acetylcholinesterase (AChE)? Implementation of assay conditions for the use of AChE activity as a biomarker of metal toxicity,” *Biomarkers*, **10**, 5, 360–375 (2005).

43. A. Jemec, T. Tišler, D. Drobne, K. Sepčić, P. Jamnik, and M. Roš, "Biochemical biomarkers in chronically metal-stressed daphnids," *Comp. Biochem. Physiol. Part C Toxicol. Pharmacol.*, **147**, 1, 61–68 (2008).

44. P. M. Reddy and G. H. Philip, "In vivo inhibition of AChE and ATPase activities in the tissues of freshwater fish, Cyprinus carpio exposed to technical grade cypermethrin," *Bull. Environ. Contam. Toxicol.*, **52**, 4, 619–626 (1994).

45. L. Guilhermino, M. N. Lacerda, A. J. A. Nogueira, and A. M. V. M. Soares, "In vitro and in vivo inhibition of Daphnia magna acetylcholinesterase by surfactant agents: possible implications for contamination biomonitoring," *Sci. Total Environ.*, **247**, 2–3, 137–141 (2000).

46. L. Guilhermino, P. Barros, M. C. Silva, and A. M. V. M. Soares, "Should the use of inhibition of cholinesterases as a specific biomarker for organophosphate and carbamate pesticides be questioned ?," *Biomarkers*, **3**, 2, 157–163 (1998).

47. R. Romani, C. Antognelli, F. Baldracchini, A. De Santis, G. Isani, E. Giovannini, and G. Rosi, "Increased acetylcholinesterase activities in specimens of Sparus auratus exposed to sublethal copper concentrations," *Chem. Biol. Interact.*, **145**, 3, 321–329 (2003).

48. I. S. Kucherenko, O. O. Soldatkin, V. M. Arkhypova, S. V. Dzyadevych, and A. P. Soldatkin, "A novel biosensor method for surfactant determination based on acetylcholinesterase inhibition," *Meas. Sci. Technol.*, **23**, 6, 065801 (2012).

49. J. Wang, C. Timchalk, and Y. Lin, "Carbon Nanotube-Based Electrochemical Sensor for Assay of Salivary Cholinesterase Enzyme Activity: An Exposure Biomarker of

Organophosphate Pesticides and Nerve Agents," *Environ. Sci. Technol.*, **42**, 7, 2688–2693 (2008).

50. K. Wang, H.-N. Li, J. Wu, C. Ju, J.-J. Yan, Q. Liu, and B. Qiu, "TiO2-decorated graphene nanohybrids for fabricating an amperometric acetylcholinesterase biosensor," *The Analyst*, **136**, 16, 3349 (2011).

51. J. Zhao, Z. Wang, J. C. White, and B. Xing, "Graphene in the Aquatic Environment: Adsorption, Dispersion, Toxicity and Transformation," *Environ. Sci. Technol.*, **48**, 17, 9995–10009 (2014).

52. K. Aschberger, H. J. Johnston, V. Stone, R. J. Aitken, C. L. Tran, S. M. Hankin, S. A. K. Peters, and F. M. Christensen, "Review of fullerene toxicity and exposure – Appraisal of a human health risk assessment, based on open literature," *Regul. Toxicol. Pharmacol.*, **58**, 3, 455–473 (2010).

53. R. H. Baughman, A. A. Zakhidov, and W. A. de Heer, "Carbon Nanotubes--the Route Toward Applications," *Science*, **297**, 5582, 787–792 (2002).

54. Q. Mu, W. Liu, Y. Xing, H. Zhou, Z. Li, Y. Zhang, L. Ji, F. Wang, Z. Si, B. Zhang, and B. Yan, "Protein Binding by Functionalized Multiwalled Carbon Nanotubes Is Governed by the Surface Chemistry of Both Parties and the Nanotube Diameter," *J. Phys. Chem. C*, **112**, 9, 3300–3307 (2008).

55. G. L. Ellman, K. D. Courtney, V. Andres jr., and R. M. Featherstone, "A new and rapid colorimetric determination of acetylcholinesterase activity," *Biochem. Pharmacol.*, **7**, 2, 88–95 (1961).

56. J. Massoulié, N. Perrier, H. Noureddine, D. Liang, and S. Bon, “Old and new questions about cholinesterases,” *Chem. Biol. Interact.*, **175**, 1–3, 30–44 (2008).

57. I. Silman and J. L. Sussman, “Acetylcholinesterase: How is structure related to function?,” *Chem. Biol. Interact.*, **175**, 1–3, 3–10 (2008).

58. M. Harel, G. Kryger, T. L. Rosenberry, W. D. Mallender, T. Lewis, R. J. Fletcher, J. M. Guss, I. Silman, and J. L. Sussman, “Three-dimensional structures of Drosophila melanogaster acetylcholinesterase and of its complexes with two potent inhibitors,” *Protein Sci.*, **9**, 6, 1063–1072 (2000).

Figure captions:

Fig. 12-1. The principle of the acetylcholinesterase (AChE) measurement according to Ellman [55].

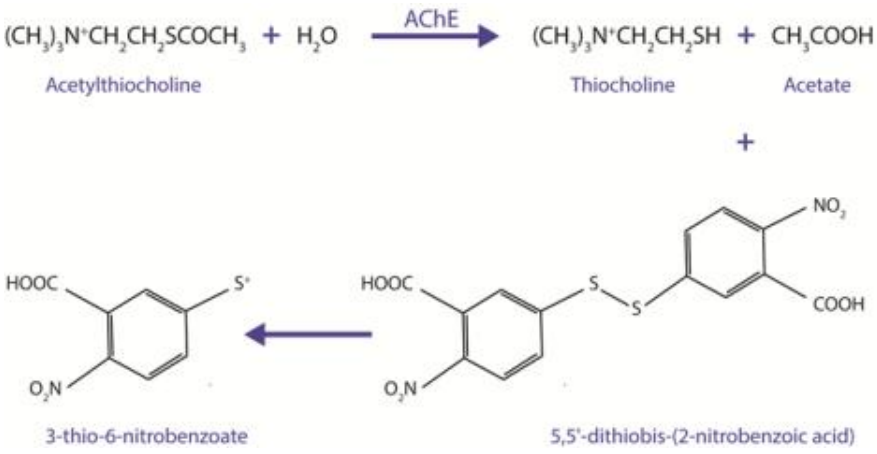

Fig. 12-1. The principle of the acetylcholinesterase (AChE) measurement according to Ellman [55].

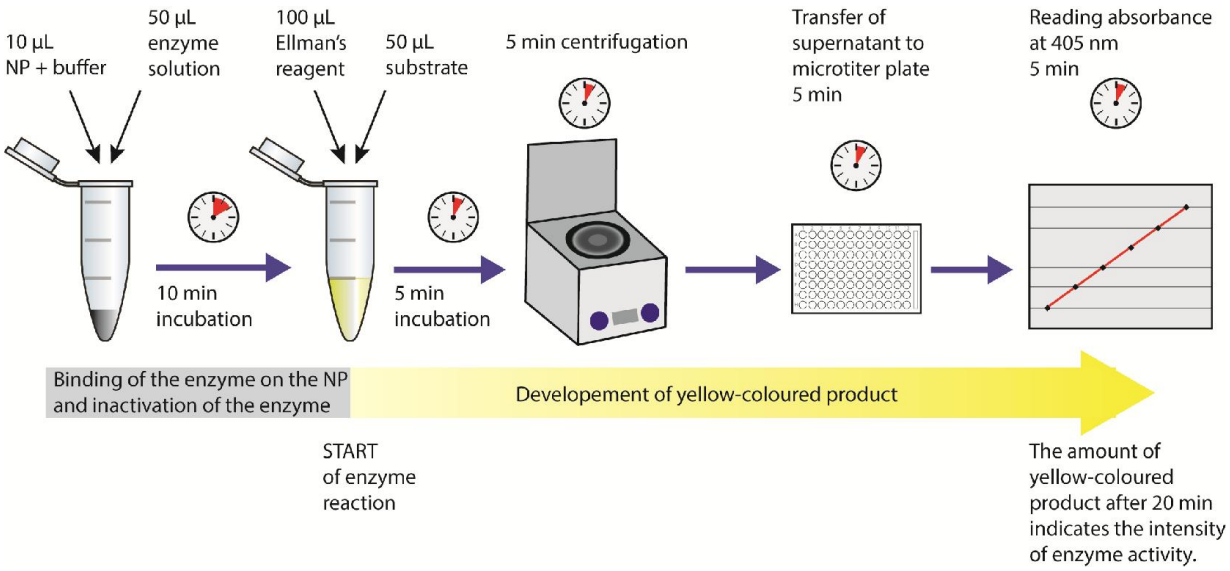

Fig. 12-2. Experimental set-up for measurement of AChE inhibition.

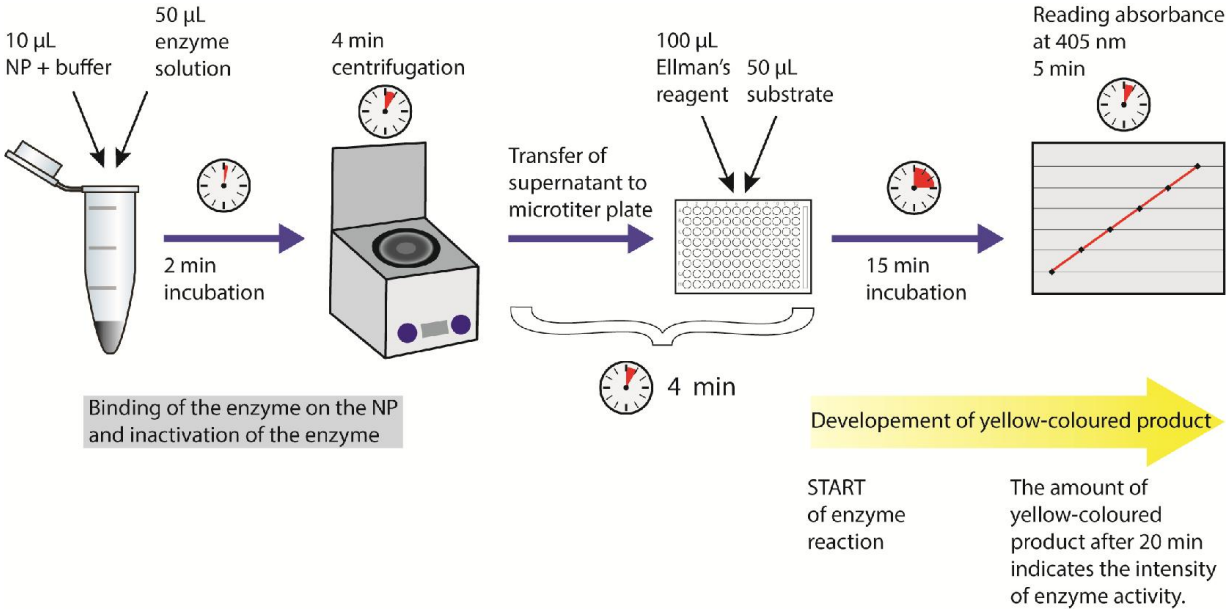

Fig. 12-3. Experimental set-up for measurement of AChE adsorption.